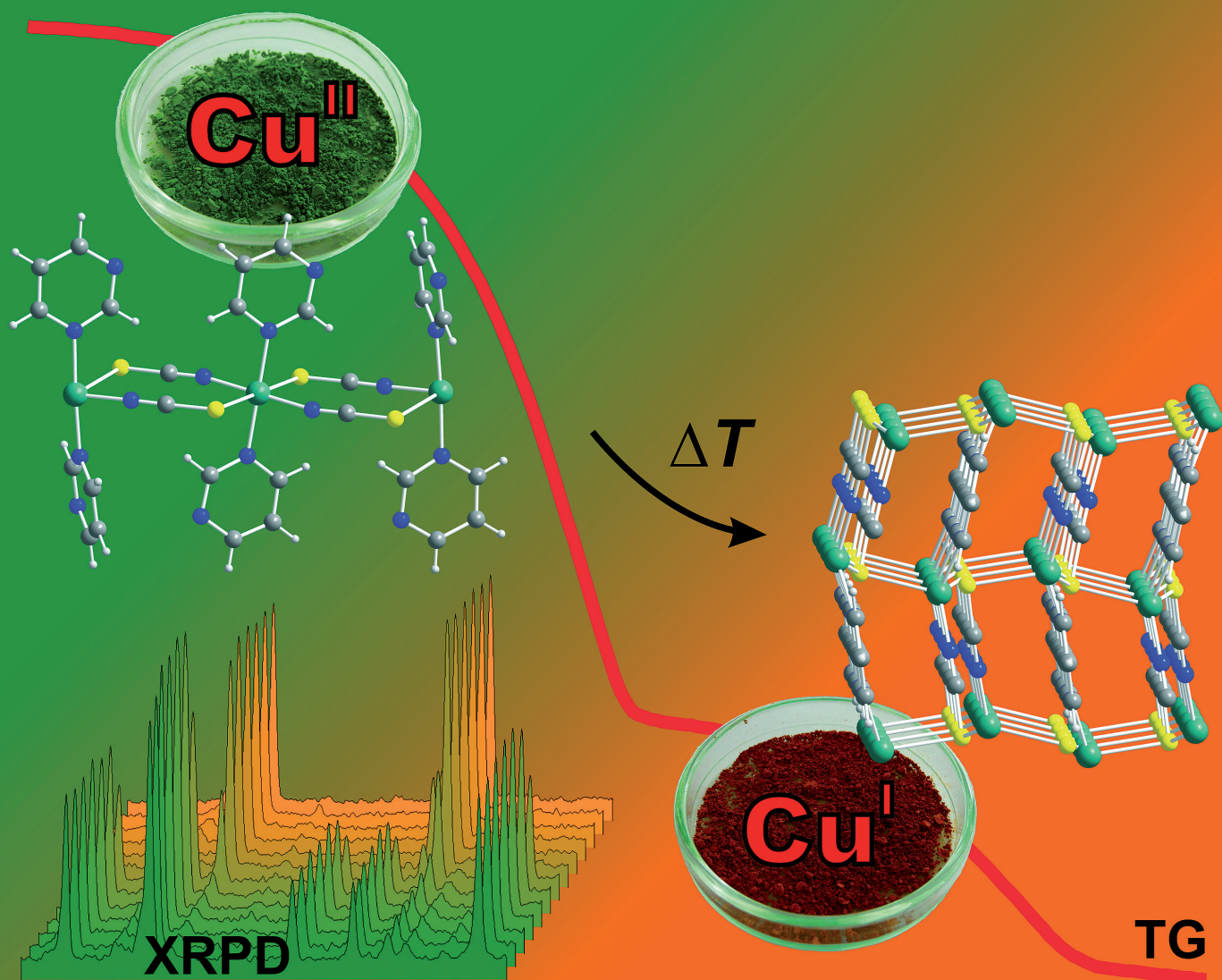


Dalton Transactions

An international journal of inorganic chemistry

www.rsc.org/dalton

Number 46 | 14 December 2009 | Pages 10125–10376



ISSN 1477-9226

RSC Publishing

PAPER

Wriedt and Näther
In situ solid state formation of copper(I)
 coordination polymers by thermal
 reduction of copper(II) precursor
 compounds

PERSPECTIVE

Duhme-Klair *et al.*
 Supramolecular interactions between
 functional metal complexes and
 proteins



1477-9226(2009)46:1-T

In situ solid state formation of copper(I) coordination polymers by thermal reduction of copper(II) precursor compounds: structure and reactivity of $[\text{Cu}(\text{NCS})_2(\text{pyrimidine})_2]_n$ [†]

Mario Wriedt and Christian Näther*

Received 19th May 2009, Accepted 14th August 2009

First published as an Advance Article on the web 28th August 2009

DOI: 10.1039/b909838k

Reaction of copper(II) thiocyanate with pyrimidine leads to the formation of the new ligand-rich 1:2 (1:2 = ratio metal salt to ligand) copper(II) compound $[\text{Cu}(\text{NCS})_2(\text{pyrimidine})_2]_n$ (**1**). Its crystal structure was determined by X-ray single crystal investigations. It consists of linear polymeric chains, in which the Cu^{2+} cations are μ -1,3 bridged by the thiocyanato anions. The pyrimidine ligands are terminal *N*-bonded to the Cu^{2+} cations, which are overall octahedrally coordinated by two pyrimidine ligands and two *N*-bonded as well as two *S*-bonded thiocyanato anions. Magnetic measurements were performed yielding weak net ferromagnetic interactions between adjacent Cu^{2+} centers mediated by the long Cu–S distances and/or interchain effects. On heating compound **1** to approx. 160 °C, two thirds of the ligands are discharged, leading to a new intermediate compound, which was identified as the ligand-deficient 2:1 copper(I) compound $[(\text{CuNCS})_2(\text{pyrimidine})]_n$ by X-ray powder diffraction. Consequently, copper(II) was reduced *in situ* to copper(I) on heating, forming polythiocyanogen as byproduct. Elemental analysis and infrared spectroscopic investigations confirm this reaction pathway. Further investigations on other ligand-rich copper(II) thiocyanato compounds clearly show that this *in situ* thermal solid state reduction works in general.

Introduction

Investigations on coordination polymers and metal–organic frameworks have achieved enormous interest during the past few decades, and have gradually become one of the most active fields in inorganic and material chemistry.¹ In most cases, these compounds were prepared in solution. This may lead to problems, because in several cases, mixtures of different phases are obtained that have to be separated by hand. Moreover, in some cases, thermodynamically metastable compounds can easily be overlooked. Thus, alternative routes for the discovery and synthesis of pure coordination polymers are required.

Recently, we proved that thermal decomposition reactions of suitable ligand-rich precursor compounds based on copper(I), silver(I), zinc(II) and cadmium(II) halides and *N*-donor ligands can be widely used as a convenient preparative tool for the facile synthesis of new pure ligand-deficient coordination compounds.² In further investigations we have shown that ligand-deficient compounds based on paramagnetic transition metals can also be prepared by this method.^{3,4} In these reactions more condensed

coordination networks are formed, which leads frequently to compounds with cooperative magnetic phenomena.^{3,4} In this project we synthesized a new ligand-rich 1:2 copper(II) thiocyanato compound with pyrimidine as ligand as a precursor for the preparation of new ligand-deficient compounds by thermal decomposition. Surprisingly, thermal decomposition leads to the formation of a ligand-deficient 2:1 copper(I) compound, which was formed by *in situ* thermal reduction of the copper(II) precursor. In the following we report these investigations.

Experimental

General

CuCl_2 , KNCS, pyrimidine, 4,4'-bipyridine and pyrazine were obtained from Alfa Aesar. $\text{Cu}(\text{NCS})_2$ was prepared by the reaction of equimolar amounts of KNCS and CuSO_4 in water. The black precipitate was filtered off immediately and washed with water. The residue was dried over concentrated H_2SO_4 . The purity of all compounds was checked by X-ray powder diffraction (see Fig. S1 to S3 in the ESI[†]) and elemental analysis.

Synthesis of catena[bis(μ_2 -thiocyanato-*N,S*)-bis(pyrimidine-*N*)-copper(II)] (**1**)

A mixture of CuCl_2 (268.9 mg, 2 mmol), KNCS (388.8 mg, 4.0 mmol) and pyrimidine (320.4 mg, 4.0 mmol) was stirred in 5 mL water at RT. After 3 days the dark green crystalline powder obtained was filtered off and washed with water, ethanol and diethyl ether and dried in air. Yield: 601.2 mg (88.4%). Calculated for $\text{C}_{10}\text{H}_8\text{CuN}_6\text{S}_2$ (339.9): C 35.34, H 2.37, N 24.73, S 18.87; found: C 35.05, H 2.31, N 24.45, S 18.61. IR (KBr): $\nu_{\text{max}} = 3426$ (b),

Institut für Anorganische Chemie, Universität zu Kiel, Max-Eyth-Straße 2, 24098, Kiel, Germany. E-mail: cnaether@ac.uni-kiel.de; Fax: +49-431-8801520; Tel: +49-431-8802092

[†] Electronic supplementary information (ESI) available: Selected bond lengths and angles for **1**; experimental and calculated XRPD patterns of compounds **1**, **2** and **3**; IR spectroscopic data of compounds **1**, **2**, **3** and all intermediates obtained in the first heating step; TG curve of compound **2**; experimental XRPD pattern of the intermediate obtained in the first heating step of compound **2** in comparison with the calculated XRPD patterns of CuNCS and $[(\text{CuNCS})_2(\text{pyrazine})]_n$. CCDC reference number 733158. For ESI and crystallographic data in CIF or other electronic format see DOI: 10.1039/b909838k

3067 (w), 2937 (w), 2099 (vs), 1630 (w), 1565 (s), 1558 (m), 1469 (m), 1405 (s), 1223 (w), 1178 (w), 1083 (w), 1015 (w), 819 (w), 707 (m), 640 (m), 481 (w) cm^{-1} (see Fig. S4 in the ESI†).

Single crystals suitable for X-ray structure determination were prepared by the reaction of CuCl_2 (33.6 mg, 0.25 mmol), KNCS (48.6 mg, 0.5 mmol) and pyrimidine (80.1 mg, 1 mmol) in 3 mL methanol at RT in a closed snap cap vial. After 1 week green block-shaped single crystals were obtained.

Synthesis of poly[bis(μ_2 -thiocyanato-*N,S*)-(4,4'-bipyridine-*N,N'*)-copper(II)] (3)

A mixture of CuCl_2 (67.2 mg, 0.5 mmol), KNCS (97.2 mg, 1 mmol) and pyrazine (40.0 mg, 0.5 mmol) was stirred in 4 mL water at RT. After 3 days the moss green crystalline powder obtained was filtered off and washed with water, ethanol and diethyl ether and dried in air. Yield: 112.1 mg (86.3%). Calculated for $\text{C}_6\text{H}_4\text{CuN}_4\text{S}_2$ (259.8): C 27.74, H 1.55, N 21.57, S 24.68; found: C 27.51, H 1.44, N 21.38, S 24.58. IR (KBr): $\nu_{\text{max}} = 3441$ (b), 3111 (w), 3090 (w), 3040 (w), 2122 (vs), 1636 (w), 1488 (w), 1414 (m), 1158 (m), 1122 (m), 1062 (m), 978 (w), 935 (w), 826 (w), 798 (m), 486 (m), 439 (w) cm^{-1} (see Fig. S5 in the ESI†).

Synthesis of poly[bis(μ_2 -thiocyanato-*N,S*)-(4,4'-bipyridine-*N,N'*)-copper(II)] (3)

A mixture of $\text{Cu}(\text{NCS})_2$ (89.9 mg, 0.5 mmol) and 4,4'-bipyridine (320.4 mg, 4.0 mmol) was stirred in a mixture of 2 mL water and 2 mL ethanol at RT. After 3 days the light green crystalline powder obtained was filtered off and washed with water, ethanol and diethyl ether and dried in air. Yield: 141.1 mg (84.0%). Calculated for $\text{C}_{12}\text{H}_8\text{CuN}_4\text{S}_2$ (335.9): C 42.91, H 2.40, N 16.68, S 19.09; found: C 42.48, H 2.24, N 16.21, S 18.88. IR (KBr): $\nu_{\text{max}} = 3431$ (b), 3073 (w), 2918 (w), 2107 (vs), 1609 (m), 1534 (w), 1491 (w), 1413 (w), 1319 (w), 1229 (m), 1072 (w), 1015 (w), 809 (m), 727 (w), 643 (w), 582 (w), 505 (w), 471 (w) cm^{-1} (see Fig. S6 in the ESI†).

Elemental analysis of the residues obtained in the thermal decomposition.

(A) Isolated after the first heating step (see Thermoanalytic Investigations) for $[\text{Cu}(\text{NCS})_2(\text{pyrimidine})_2]_n$ (1). Calculated for $\{[\text{Cu}(\text{NCS})_2]_2(\text{pyrimidine})_2\}_n$: C 21.86, H 0.92, N 19.12, S 29.18; found C 21.86, H 1.03, N 18.92, S 28.58. (B) Isolated after the first heating step for $[\text{Cu}(\text{NCS})_2(\text{pyrazine})]_n$ (2). Calculated for $[(\text{Cu}(\text{NCS})_2(\text{pyrazine}))_n + (\text{NCS})_2]$: C 21.86, H 0.92, N 19.12, S 29.18; found C 19.90, H 0.62, N 17.85, S 31.15. (C) Isolated after the first heating step for $[\text{Cu}(\text{NCS})_2(4,4'\text{-bipyridine})]_n$ (3). Calculated for $[(\text{Cu}(\text{NCS})_2(4,4'\text{-bipyridine}))_n + (\text{NCS})_2]$: C 32.61, H 1.56, N 16.30, S 24.88; found C 32.74, H 1.66, N 16.22, S 24.75.

Single-crystal structure analysis

The investigation was performed with an imaging plate diffraction system (IPDS-1) with $\text{Mo-K}\alpha$ -radiation from STOE & CIE. The structure solution was performed by direct methods using SHELXS-97,⁵ and structure refinements were performed against F^2 using SHELXL-97.⁶ The crystal was pseudo merohedral

Table 1 Selected crystal data and details on the structure determination from single crystal data for **1**

Compound	$[\text{Cu}(\text{NCS})_2(\text{pyrimidine})_2]_n$
formula	$\text{C}_{10}\text{H}_8\text{CuN}_6\text{S}_2$
MW/g mol ⁻¹	339.88
crystal system	triclinic
space group	<i>P</i> -1
<i>a</i> /Å	9.3335(7)
<i>b</i> /Å	9.3730(7)
<i>c</i> /Å	17.1942(13)
α /deg	97.879(9)
β /deg	97.745(9)
γ /deg	115.761(8)
<i>V</i> /Å ³	1309.69(17)
<i>T</i> /K	170
<i>Z</i>	4
<i>D</i> _{calc} /g cm ⁻³	1.724
μ /mm ⁻¹	1.980
min/max transmission	0.798/0.849
θ_{max} /deg	26.02
measured reflections	10205
unique reflections	4967
reflections [$F_o > 4\sigma(F_o)$]	4258
parameter	348
<i>R</i> _{int}	0.0354
<i>R</i> ₁ ^a [$F_o > 4\sigma(F_o)$]	0.0310
<i>wR</i> ₂ ^b [all data]	0.0781
GOF	0.984
$\Delta\rho_{\text{max}}, \Delta\rho_{\text{min}}$ /e Å ⁻³	0.484, -0.589

$$^a R_1 = \sum \|F_o\| - |F_c| / \sum \|F_o\| \cdot ^b wR_2 = [\sum [w(F_o^2 - F_c^2)^2] / \sum [w(F_o^2)^2]]^{1/2}$$

twinned around a 2-fold rotation axis and therefore a twin refinement was performed using the TWIN option in SHELXL-97⁶ [twin matrix: (0 -1 0) (-1 0 0) (0 0 -1); BASF: 0.243(2)]. An empirical absorption correction was applied using Platon.⁷ All non-hydrogen atoms were refined with anisotropic displacement parameters. The hydrogen atoms were positioned with idealized geometry and were refined with fixed isotropic displacement parameters [$U_{\text{eq}}(\text{H}) = -1.2U_{\text{eq}}(\text{C})$] using a riding model with $d_{\text{C-H}} = 0.95$ Å. Details of the structure determination are given in Table 1.

X-ray powder diffraction (XRPD)

XRPD experiments were performed using a Stoe Transmission Powder Diffraction System (STADI P) with $\text{Cu-K}\alpha$ -radiation ($\lambda = 154.0598$ pm) that is equipped with a linear position-sensitive detector (Delta 2 Theta = 6.5–7° simultaneous; scan range overall = 2–130°) from STOE & CIE.

Differential thermal analysis, thermogravimetry, and mass spectroscopy (DTA-TG-MS)

The DTA-TG measurements were performed in a nitrogen atmosphere (purity: 5.0) in Al_2O_3 crucibles using a STA-409CD instrument from Netzsch. The DTA-TG-MS measurements were performed with the same instrument, which is connected to a quadrupole mass spectrometer from Balzers *via* Skimmer coupling from Netzsch. The MS measurements were performed in analogue and trend scan modes in Al_2O_3 crucibles in a dynamic helium atmosphere (purity: 5.0) using heating rates of 4 °C/min. All measurements were performed with a flow rate of 75 mL/min and

were corrected for buoyancy and current effects. The instrument was calibrated using standard reference materials.

Elemental analysis

CHNS analyses were performed using an EURO EA elemental analyzer, fabricated by EURO VECTOR Instruments and Software.

Spectroscopy

Fourier transform IR spectra were recorded on a Genesis series FTIR spectrometer, by ATI Mattson, in KBr pellets.

Magnetic measurement

The magnetic measurement was performed using a Physical Property Measuring System (PPMS) from Quantum Design, which is equipped with a 9 T magnet. The data were corrected for core diamagnetism.⁸

Results and discussion

Crystal structure

The ligand-rich 1:2 compound $[\text{Cu}(\text{NCS})_2(\text{pyrimidine})_2]_n$ (**1**) crystallizes in the centrosymmetric triclinic space group $P\bar{1}$ with four formula units in the unit cell (Table 1). The asymmetric unit consists of two metal cations located on centers of inversion as well as one metal cation, four thiocyanato anions and four pyrimidine ligands in the general position. In the crystal structure the metal cations are coordinated by two pyrimidine ligands, two S and two N atoms of four thiocyanato anions within a slightly distorted octahedral geometry (Fig. 1).

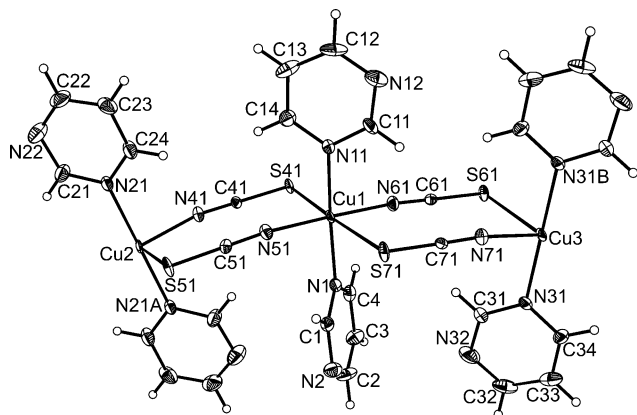


Fig. 1 Crystal structure of $[\text{Cu}(\text{NCS})_2(\text{pyrimidine})_2]_n$ (**1**) with a view of the coordination sphere of the Cu^{2+} cations with labeling and displacement ellipsoids drawn at the 50% probability level. Symmetry codes: A = $-x + 1, -y + 2, -z + 1$; B = $-x - 1, -y, -z$.

The Cu^{2+} cations are each μ -1,3 bridged by four thiocyanato anions, resulting in the formation of linear polymeric $\text{Cu}(\text{NCS})_2$ -Cu chains, in which the pyrimidine ligands are terminal N-bonded to the Cu^{2+} cations (Fig. 2: top). This chains consist of two alternating types of Cu^{2+} coordination polyhedra, linked by the thiocyanato anions: one with pyrimidine ligands forming a dihedral angle of $88.2(5)^\circ$ at Cu1 and the other due to symmetry

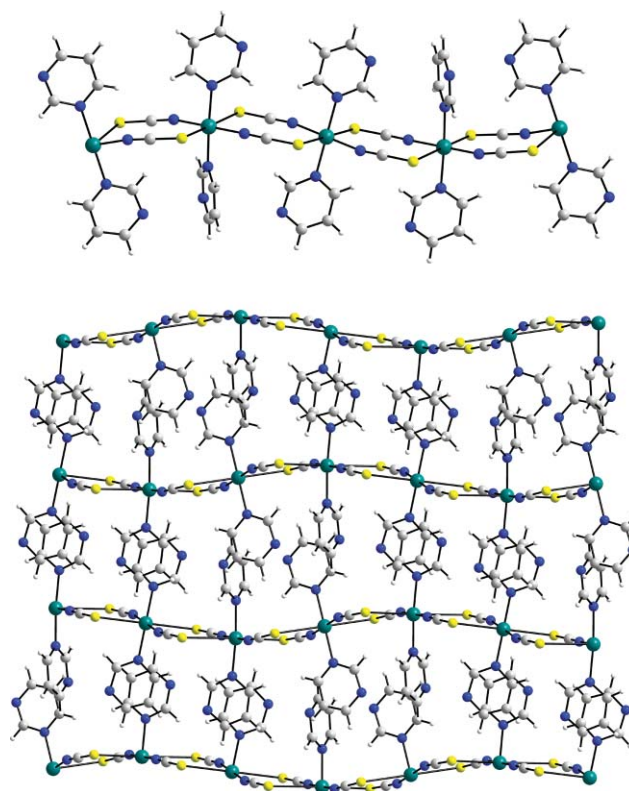


Fig. 2 Extended crystal structure of $[\text{Cu}(\text{NCS})_2(\text{pyrimidine})_2]_n$ (**1**) with a view of the intramolecular chains (top) and its intermolecular layers with a view along the c -axis (bottom).

with coplanar pyrimidine ligands at Cu2 and Cu3. Overall this topology is not unusual for monodentate pyridyl derivatives.⁹ However, in contrast to other ligand-rich 1:2 thiocyanato compounds based on the bidentate pyrimidine as ligand a topology is found, in which the thiocyanato anions are terminal N-bonded and the metal centers are bridged by the pyrimidine ligands into layers.^{4,10} The shortest centroid-centroid distance of two adjacent terminal bonded parallel pyrimidine ligands amounts to $3.774(1)$ Å, which indicates π - π -interactions. If these interactions were taken into account, the structure of **1** can be described as a 3D network containing layers, which are stacked perpendicular to the crystallographic c -axis (Fig. 2: bottom).

The Cu-NCS distances range between $1.930(3)$ and $1.957(3)$ Å and the Cu-SCN distances range between $2.808(1)$ and $3.115(1)$ Å. The octahedral coordination around the Cu^{2+} cations is slightly distorted with angles of $88.98(13)$ to $93.19(9)^\circ$ as well as $174.86(12)$ to 180° . The almost linear thiocyanato anions form with the Cu^{2+} cations Cu-S-CN angles of about $95.2(1)$ to $98.2(1)^\circ$ and Cu-N-CS angles of about $168.1(3)$ to $173.2(3)^\circ$ (see Table S1 in the ESI†). The metal-metal separation through the thiocyanato anions amounts to $5.679(1)$ and $5.777(1)$ Å, whereas the shortest interchain as well as the shortest interlayer separation of two adjacent metal cations amounts to $8.386(8)$ and $8.376(9)$ Å.

Magnetic investigations

In compound **1** the copper(II) cations are μ -1,3 bridged by the thiocyanato anions, which can lead to magnetic exchange

interactions. Several similar copper(II) compounds were investigated for their magnetic properties, which were described as weak antiferromagnetic interactions.¹¹

To investigate the magnetic properties in compound **1**, the temperature dependence of the magnetic susceptibility was investigated by applying a magnetic field of $H = 1$ T in the temperature range 300–2 K. The magnetic data were fitted according to the Curie–Weiss law $\chi_M = C/(T - \theta)$ in the temperature range 150–2 K with $\theta = 1.00$ K and $C = 0.3732$ K cm³ mol⁻¹. In the high temperature range a fitting was not performed, because the susceptibility signal was too low. The effective magnetic moment μ_{eff} of 1.73 μ_B is in exact agreement with the spin-only value of 1.73 μ_B for a high spin Cu²⁺ ion ($S = \frac{1}{2}$, $g = 2.0$). The overall paramagnetic Curie–Weiss behavior (Fig. 3: top) yielding a small positive Weiss constant, indicating net ferromagnetic interactions between the Cu²⁺ centers on cooling, attributed to the long Cu–S distances and/or interchain effects. This is also obvious by the increase of the $\chi_M T$ values upon cooling to a maximum value of 40.65 K cm³ mol⁻¹ at 15.5 K (Fig. 3: bottom) due to increasing ferromagnetic correlations between adjacent spin carriers. Upon cooling to 2 K, $\chi_M T$ decreases quickly due to rapidly increasing antiferromagnetic interactions.

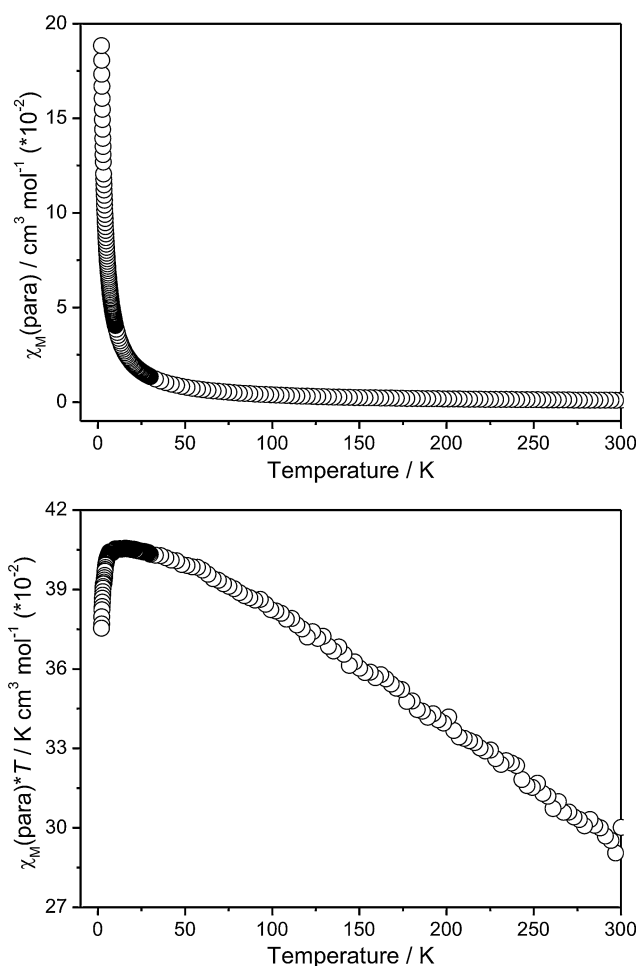


Fig. 3 Results of the magnetic measurement by plots of paramagnetic susceptibility (top) and $\chi_M T$ (bottom) as a function of temperature for $[\text{Cu}(\text{NCS})_2(\text{pyrimidine})_2]_n$ (**1**).

Investigations on the thermal decomposition reaction

On heating, the ligand-rich 1:2 compound $[\text{Cu}(\text{NCS})_2(\text{pyrimidine})_2]_n$ (**1**) in a thermobalance up to 400 °C, two mass steps are observed in the TG curve that are accompanied with endothermic events in the DTA curve. The DTG curve shows that these events are well separated (Fig. 4). From the MS trend scan curve, it is proven that only the ligand pyrimidine ($m/z = 80$) is lost during these mass steps. The experimental mass loss of 35.2% in the first step is in perfect agreement with that calculated for the release of three-quarter of the ligands ($\Delta m_{\text{theo}}(-\frac{3}{4} \cdot \text{pyrimidine}) = 35.3\%$) and the experimental mass loss of 11.4% in the second step corresponds very good to the loss of the rest of the ligands ($\Delta m_{\text{theo}}(-\frac{1}{4} \cdot \text{pyrimidine}) = 11.8\%$).

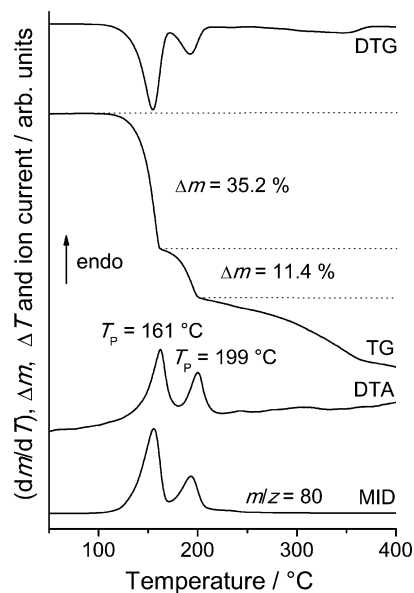


Fig. 4 DTG, TG, DTA and MS trend scan curves for the ligand-rich 1:2 compound $[\text{Cu}(\text{NCS})_2(\text{pyrimidine})_2]_n$ (**1**). Heating rate = 4 °C/min; $m/z = 80$ (pyrimidine); given are the mass changes (%) and the peak temperatures T_p (°C).

Based on the experimental mass losses, it can be assumed that in the first heating step a ligand-deficient 2:1 compound of composition $[\{\text{Cu}(\text{NCS})_2\}_2(\text{pyrimidine})_n]$ is formed. On further heating, the remaining ligands are lost leading to the formation of $\text{Cu}(\text{NCS})_2$, which decomposes on further heating.

In order to verify the nature of the first intermediate formed, additional TG measurements with heating rates of 4 °C/min were performed and stopped after the first TG step. The residue obtained was investigated by elemental analysis, X-ray powder diffraction and magnetic measurements. Elemental analysis (see Experimental section) is in good agreement with that calculated for the copper(II) compound $[\{\text{Cu}(\text{NCS})_2\}_2(\text{pyrimidine})_n]$ and the XRPD pattern suggests a phase pure compound (Fig. 5A). Surprisingly, magnetic measurements show that a diamagnetic copper(I) compound was formed. Based on this result we identified the intermediate as the ligand-deficient 2:1 copper(I) compound $[(\text{CuNCS})_2(\text{pyrimidine})_n]$, reported recently (compare A with B in Fig. 5).¹²

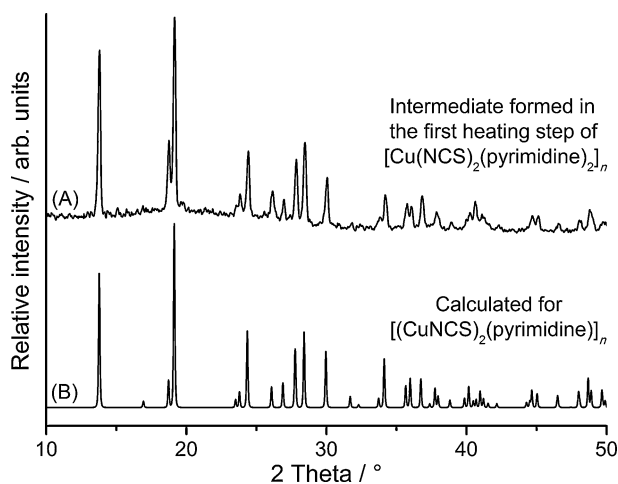


Fig. 5 Experimental XRPD pattern of the residue obtained in the first heating step in the thermal decomposition reaction of the ligand-rich 1:2 compound $[\text{Cu}(\text{NCS})_2(\text{pyrimidine})_2]_n$ (**1**) (A) and calculated XRPD pattern of the ligand-deficient 2:1 compound $[(\text{CuNCS})_2(\text{pyrimidine})]_n$ (B) from single crystal data.

To verify the decomposition process of compound **1** in more detail, additional temperature-dependent X-ray powder diffraction experiments were carried out. These measurements confirm the *in situ* thermal reduction of compound **1** into a copper(I) species and do not show any additional ligand-deficient intermediates (Fig. 6).

The elemental analysis of the intermediate formed in the first heating step is in disagreement with that calculated for the copper(I) species $[(\text{CuNCS})_2(\text{pyrimidine})]_n$ as proved by XRPD, but well suited to the copper(II) species $\{[\text{Cu}(\text{NCS})_2]_2(\text{pyrimidine})\}_n$ (see Experimental section). Therefore, we assume that copper(II) thiocyanate decomposes by an *in situ* reduction to copper(I) thiocyanate and amorphous thiocyanogen, a reaction which was reported recently.^{13,14}



Thiocyanogen $(\text{NCS})_2$ is thermally unstable and polymerises spontaneously to give an orange/brick-red solid product of polythiocyanogen $(\text{NCS})_x$.¹⁵ To confirm this assumption additional infrared spectroscopic investigations were carried out, which show a very sharp band at 2124 cm^{-1} and a very broad band around 1199 cm^{-1} (see Fig. S7 in the ESI†). The first band agrees with the C–N stretching vibration of the thiocyanato anion, which occurs in μ -1,3 bridging thiocyanato compounds well above 2100 cm^{-1} ,¹⁶ whereas the second one accords to ring vibrations of polythiocyanogen.^{13,15} Experiments to remove the byproduct polythiocyanogen by dissolving with various solvents were unsuccessful.

A general behavior?—thermal decomposition of other copper(II) thiocyanato compounds

To prove if other ligand deficient copper(I) thiocyanato coordination compounds can be prepared by *in situ* reduction of copper(II) precursor compounds, we investigated other potential ligand rich copper(II) coordination compounds for their thermal properties. A search in the Cambridge Crystal Structure Database yields two potential ligand-rich copper(II) thiocyanato compounds based on 4,4'-bipyridine¹⁷ and pyrazine¹⁸ as ligands, for which also corresponding ligand-deficient copper(I) compounds were reported recently.^{19,20} Thus, we investigated both ligand-rich copper(II) compounds for their thermal properties:

On heating the ligand-rich 1:1 copper(II) compound $[\text{Cu}(\text{NCS})_2(\text{pyrazine})]_n$ (**2**), two mass steps are observed in the TG curve, of which each step corresponds to the removal of half of the pyrazine ligands (see Fig. S10 in the ESI†). XRPD investigations of the residue obtained in the first heating step show clearly that the ligand-deficient 2:1 copper(I) compound $[(\text{CuNCS})_2(\text{pyrazine})]_n$ ¹⁹ was formed (see Fig. S11 in the ESI†). IR spectroscopic investigations (see Fig. S8 in the ESI†) and elemental analysis (see Experimental section) supports this finding with polythiocyanogen as byproduct. It must be noted that the two mass steps are not well resolved and therefore, the

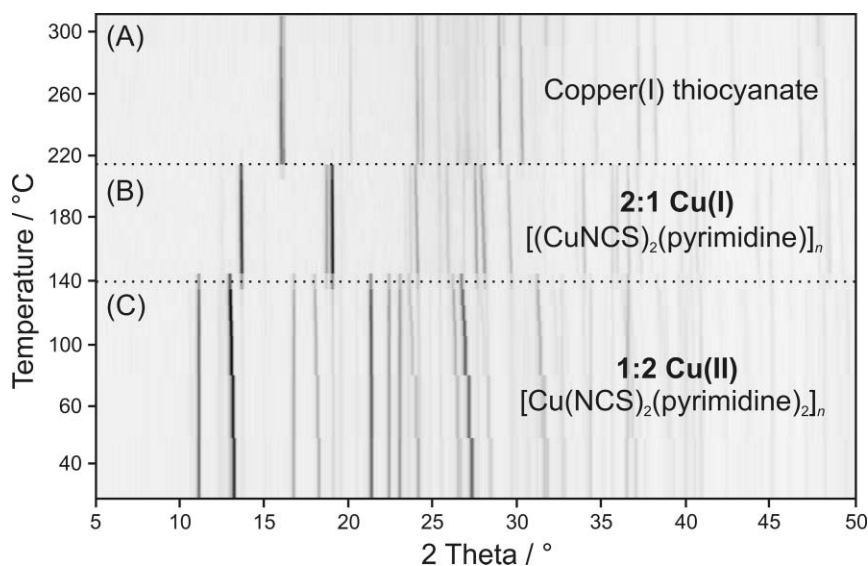


Fig. 6 Temperature-dependent XRPD pattern of the ligand-rich 1:2 compound $[\text{Cu}(\text{NCS})_2(\text{pyrimidine})_2]_n$ (**1**) (C), which decomposes into the ligand-deficient 2:1 compound $[(\text{CuNCS})_2(\text{pyrimidine})]_n$ (B) and copper(I) thiocyanate (A).

intermediate is contaminated with small amounts of copper(I) thiocyanate.

For the ligand-rich 1:1 copper(II) compound $[\text{Cu}(\text{NCS})_2(4,4'\text{-bipyridine})]_n$ (**3**), also two mass steps are observed in the TG curve (Fig. 7: top). The experimental X-ray powder pattern of the residue formed in the first step is in good agreement with that calculated for the ligand-deficient 2:1 copper(I) compound $[(\text{CuNCS})_2(4,4'\text{-bipyridine})]_n$,²⁰ from single crystal data (Fig. 7: bottom). IR spectroscopic investigations (see Fig. S9 in the ESI†) and elemental analysis (see Experimental section) support this finding. Surprisingly, the XRPD investigations show clearly that the ligand deficient 2:1 copper(I) compound is contaminated with small amounts of the ligand-rich 1:1 copper(I) compound $[\text{CuNCS}(4,4'\text{-bipyridine})]_n$,²¹ in which the ratio between copper and the ligands is identical to that in the precursor. This indicates that the reduction takes place before the ligands are emitted, which means that copper(I) coordination polymers might also be prepared without loss of the organic ligands.

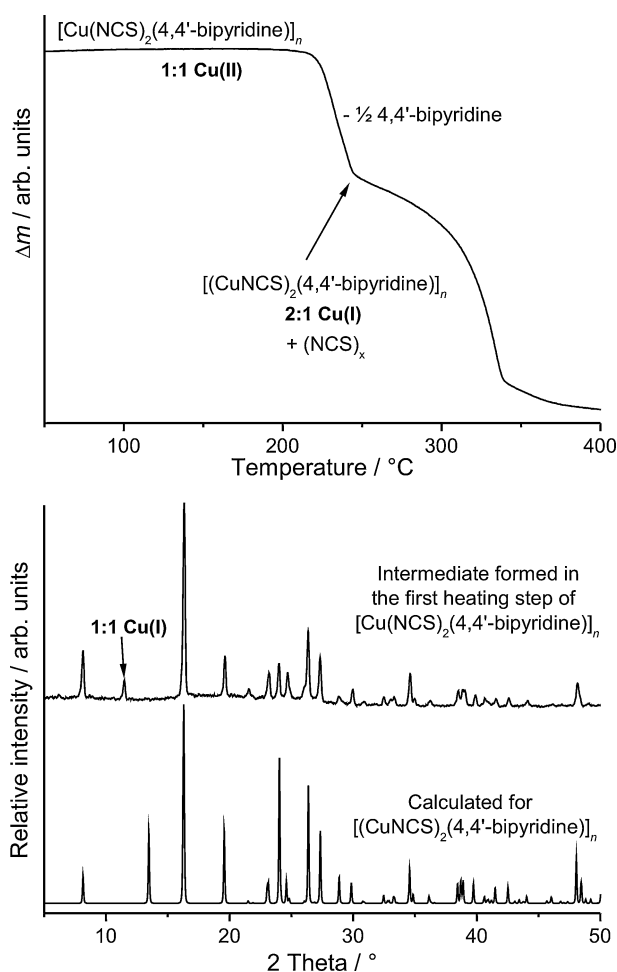


Fig. 7 TG curve of the ligand-rich 1:1 compound $[\text{Cu}(\text{NCS})_2(4,4'\text{-bipyridine})]_n$,¹⁷ (**3**) (top) and experimental XRPD pattern of the intermediate obtained in the first heating step of compound **3** as well as the calculated XRPD pattern for the ligand-deficient 2:1 compound $[(\text{CuNCS})_2(4,4'\text{-bipyridine})]_n$ from single crystal data (bottom).

Conclusion

In this contribution we reported on the preparation and characterization of the new ligand-rich 1:2 copper(II) compound $[\text{Cu}(\text{NCS})_2(\text{pyrimidine})_2]_n$. In its crystal structure the Cu^{2+} cations are coordinated by two *N*-bonded pyrimidine ligands and two *S*-bonded as well as two *N*-bonded thiocyanato anions in an octahedral geometry. The Cu^{2+} cations are each μ -1,3 bridged by four thiocyanato anions, resulting in the formation of linear polymeric $\text{Cu}-(\text{NCS})_2-\text{Cu}$ chains, in which the pyrimidine ligands are terminal *N*-bonded to the Cu^{2+} cations. We also proved that on heating in this compound an *in situ* thermal reduction takes place, in which the Cu^{2+} cations are reduced by a part of the thiocyanato anions, which are oxidized to amorphous polythiocyanogen as a byproduct.

Furthermore we showed that this *in situ* thermal solid state reduction works in general: ligand-rich copper(II) thiocyanato compounds based on 4,4'-bipyridine and pyrazine as ligands also transform into the corresponding ligand-deficient copper(I) thiocyanato compounds. Even if this is an unexpected redox reaction in the solid state, this method cannot so far be used as a synthetic tool for the synthesis of new ligand-deficient copper(I) thiocyanato compounds, because polythiocyanogen is formed as a byproduct. This would be different, if the polythiocyanogen could be removed. However, the formation of $(\text{NCS})_x$ and $(\text{NCS})_x$ proceeds *via* SCN^\bullet radicals.¹⁵ Thus, suitable scavengers need to be found which could transform the radicals into a compound, which could then be separated from the copper(I) coordination compound. Such experiments will be the subject of further investigation.

Acknowledgements

Mario Wriedt thanks the *Stiftung Stipendien-Fonds des Verbandes der Chemischen Industrie* and the *Studienstiftung des deutschen Volkes* for a PhD scholarship. Moreover we gratefully acknowledge financial support by the State of Schleswig-Holstein and we thank Professor Dr. Wolfgang Bensch for access to his experimental facility. Special thanks to Inke Jeß for her support in the single crystal measurements.

References

- (a) A. J. Blake, N. R. Champness, P. Hubberstey, W.-S. Li, M. A. Withersby and M. Schröder, *Coord. Chem. Rev.*, 1999, **183**, 117–138; (b) D. Braga, L. Maini, M. Polito, L. Scaccianoce, G. Cojazzi and F. Grepioni, *Coord. Chem. Rev.*, 2001, **216–217**, 225–248; (c) C. Janiak, *Dalton Trans.*, 2003, 2781–2804; (d) S. Kitagawa and R. Matsuda, *Coord. Chem. Rev.*, 2007, **251**, 2490–2509; (e) S. Kitagawa and K. Uemura, *Chem. Soc. Rev.*, 2005, **34**, 109–119; (f) D. Maspoch, D. Ruiz-Molina and J. Veciana, *J. Mater. Chem.*, 2004, **14**, 2713–2723; (g) D. Maspoch, D. Ruiz-Molina and J. Veciana, *Chem. Soc. Rev.*, 2007, **36**, 770–818; (h) B. Moulton and M. J. Zaworotko, *Chem. Rev.*, 2001, **101**, 1629–1658; (i) R. J. Puddephatt, *Coord. Chem. Rev.*, 2001, **216–217**, 313–332; (j) A. Y. Robin and K. M. Fromm, *Coord. Chem. Rev.*, 2006, **250**, 2127–2157.
- (a) G. Bhosekar, I. Jeß and C. Näther, *Inorg. Chem.*, 2006, **45**, 6508–6515; (b) C. Näther and A. Beck, *Z. Naturforsch.*, 2004, **59b**, 992–998; (c) C. Näther, G. Bhosekar and I. Jeß, *Inorg. Chem.*, 2007, **46**, 8079–8087; (d) C. Näther and I. Jeß, *Eur. J. Inorg. Chem.*, 2004, 2868–2876; (e) C. Näther and I. Jeß, *Inorg. Chem.*, 2003, **42**, 2968–2976; (f) C. Näther, I. Jeß and J. Greve, *Polyhedron*, 2001, **20**, 1017–1022; (g) C. Näther, I. Jeß, N. Lehnert and D. Hinz-Hübner, *Solid State Sci.*, 2003, **5**, 1343–1357; (h) C. Näther, M. Wriedt and I. Jeß, *Inorg. Chem.*, 2003,

- 42, 2391–2397; (i) M. Wriedt, I. Jeß and C. Näther, *Eur. J. Inorg. Chem.*, 2009, 363–372.
- 3 (a) C. Näther and J. Greve, *J. Solid State Chem.*, 2003, **176**, 259–265; (b) M. Wriedt, I. Jeß and C. Näther, *Eur. J. Inorg. Chem.*, 2009, 1406–1413; (c) M. Wriedt and C. Näther, *Z. Anorg. Allg. Chem.*, 2009, **635**(8), 1115 in press; (d) M. Wriedt, S. Sellmer and C. Näther, *Dalton Trans.*, 2009, DOI: 10.1039/b907645j in press.
- 4 M. Wriedt, S. Sellmer and C. Näther, *Inorg. Chem.*, 2009, **48**(14), 6896 in press.
- 5 G. M. Sheldrick, *SHELXS-97, Program for Crystal Structure Solution*, University of Göttingen, Göttingen, Germany, 1997.
- 6 G. M. Sheldrick, *SHELXL-97, Program for the Refinement of Crystal Structures*, University of Göttingen, Göttingen, Germany, 1997.
- 7 A. L. Spek, Utrecht University, Utrecht, Netherlands, Editon edn., 2005.
- 8 G. A. Bain and J. F. Berry, *J. Chem. Educ.*, 2008, **85**, 532–536.
- 9 (a) G. Chen, Z.-P. Bai and S.-J. Qu, *Acta Crystallogr., Sect. E: Struct. Rep. Online*, 2005, **E61**, m2718–m2719; (b) M. Kabesová, M. Dunaj-Jurco and J. Soldánová, *Inorg. Chim. Acta*, 1987, **130**, 105–111.
- 10 F. Lloret, G. D. Munno, M. Julve, J. Cano, R. Ruiz and A. Caneschi, *Angew. Chem., Int. Ed.*, 1998, **37**, 135–138.
- 11 (a) C. Diaz, J. Ribas, N. Sanz, X. Solans and M. Font-Bardía, *Inorg. Chim. Acta*, 1999, **286**, 169–174; (b) S. Ferlay, G. Francese, H. W. Schmalte and S. Decurtins, *Inorg. Chim. Acta*, 1999, **286**, 108–113; (c) H. Grove, M. Julve, F. Lloret, P. E. Kruger, K. W. Tornroos and J. Sletten, *Inorg. Chim. Acta*, 2001, **325**, 115–124; (d) M. Julve, M. Verdaguer, G. Demunno, J. A. Real and G. Bruno, *Inorg. Chem.*, 1993, **32**, 795–802; (e) Z. E. Serna, R. Cortés, M. K. Urriaga, M. G. Barandika, L. Lezama, M. I. Arriortua and T. Rojo, *Eur. J. Inorg. Chem.*, 2001, 865–872; (f) R. Vicente, A. Escuer, E. Penalba, X. Solans and M. FontBardia, *Inorg. Chim. Acta*, 1997, **255**, 7–12.
- 12 S. A. Barnett, A. J. Blake, N. R. Champness and C. Wilson, *CrystEngComm*, 2000, **2**, 36–40.
- 13 J. A. Hunter, W. H. S. Massie, J. Meiklejohn and J. Reid, *Inorg. Nucl. Chem. Lett.*, 1969, **5**, 1–4.
- 14 B. Ptaszynski, E. Skiba and J. Krystek, *J. Therm. Anal. Calorim.*, 2001, **65**, 231–239.
- 15 W. R. Bowman, C. J. Burchell, P. Kilian, A. M. Z. Slawin, P. Wormald and J. D. Woollins, *Chem.–Eur. J.*, 2006, **12**, 6366–6381.
- 16 R. A. Bailey, S. L. Kozak, T. W. Michelsen and W. N. Mills, *Coord. Chem. Rev.*, 1971, **6**, 407–445.
- 17 W.-X. Luo, M.-M. Yu, L. Zheng, A.-L. Cui and H.-Z. Kou, *Acta Crystallogr., Sect. E: Struct. Rep. Online*, 2006, **E62**(10), m2532–m2534.
- 18 H. N. Bordallo, L. Chapon, J. L. Manson, C. D. Ling, J. S. Qualls, D. Hall and D. N. Argyriou, *Polyhedron*, 2003, **22**, 2045–2049.
- 19 A. J. Blake, N. R. Champness, M. Crew, L. R. Hanton, S. Parsons and M. Schröder, *J. Chem. Soc., Dalton Trans.*, 1998, (10), 1533–1534.
- 20 A. J. Blake, N. R. Brooks, N. R. Champness, M. Crew, L. R. Hanton, P. Hubberstey, S. Parsons and M. Schröder, *J. Chem. Soc., Dalton Trans.*, 1999, (16), 2813–2817.
- 21 M. Wriedt, S. Sellmer and C. Näther, *Acta Crystallogr., Sect. E: Struct. Rep. Online*, 2008, **E64**(11), m1424–m1425.